Lithos 230 (2015) 133–145

Contents lists available at ScienceDirect

Lithos

journal homepage: www.elsevier.com/locate/lithos

Overlapping Sr–Nd–Hf–O isotopic compositions in Permian mafic enclaves and host granitoids in Alxa Block, NW China: Evidence for crust–mantle interaction and implications for the generation of silicic igneous provinces

Wei Dan [a,b,*], Qiang Wang [a,c,*], Xuan-Ce Wang [d], Yu Liu [b], Derek A. Wyman [e], Yong-Sheng Liu [f]

[a] State Key Laboratory of Isotope Geochemistry, Guangzhou Institute of Geochemistry, Chinese Academy of Sciences, Guangzhou, Guangdong 510640, China
[b] State Key Laboratory of Lithospheric Evolution, Institute of Geology and Geophysics, Chinese Academy of Sciences, Beijing 100029, China
[c] CAS Center for Excellence in Tibetan Plateau Earth Sciences, Beijing 100101, China
[d] Department of Applied Geology, Curtin University, Perth, WA 6845, Australia
[e] School of Geosciences, The University of Sydney, NSW 2006, Australia
[f] State Key Laboratory of Geological Processes and Mineral Resources, Faculty of Earth Sciences, China University of Geosciences, Wuhan 430074, China

ARTICLE INFO

Article history:
Received 5 December 2014
Accepted 20 May 2015
Available online 2 June 2015

Keywords:
Enclave
Zircon Hf–O isotopes
Magma mixing
Crustal growth
Permian
Alxa Block

ABSTRACT

In general, the mantle provides heat and/or material for the generation of the silicic igneous provinces (SIPs). The rarity of mafic microgranular enclaves (MMEs), however, hampers understanding of the mantle's role in generating SIPs and the process of crust–mantle interaction. The widespread distributed MMEs in the newly reported Alxa SIP provide an opportunity to study these processes. This study integrates in situ zircon U–Pb age and Hf–O isotope analyses, whole-rock geochemistry and Sr–Nd isotope results for the MMEs and host granitoids in the Alxa Block. SIMS zircon U–Pb dating reveals that there are two generations of MMEs and host granitoids. The MMEs in the Bayannuoergong batholith were formed at ca. 278 Ma, similar to the age (280 Ma) of host granitoids, and the MMEs and host granitoids in the Yamaitu pluton were formed at ca. 272–270 Ma. All MMEs have relatively low SiO_2 (50.7–61.4 wt.%) and Th (0.8–2.8 ppm), but relatively high MgO (2.6–4.9 wt.%), Cr (23–146 ppm) and Ni (6–38 ppm) contents compared to the host granitoids, with SiO_2 (63.6–77.5 wt.%), Th (5.2–41 ppm), MgO (0.23–2.1 wt.%), Cr (10–38 ppm) and Ni (5–14 ppm). All MMEs have whole rock Sr–Nd and zircon Hf–O isotope compositions similar to their corresponding host granitoids. The 280 Ma MMEs have lower whole rock $\varepsilon_{Nd}(t)$ (−13.5) and higher initial $^{87}Sr/^{86}Sr$ values (0.7095) and zircon $\delta^{18}O$ values (6.3‰) compared to the $\varepsilon_{Nd}(t)$ (−11.5), initial $^{87}Sr/^{86}Sr$ values (0.7070) and zircon $\delta^{18}O$ values (5.6‰) of the 270 Ma MMEs. The occurrences of quartz xenocrysts, K-feldspar megacrysts, corroded feldspars and acicular apatites indicate that the MMEs are the products of the mixing between mantle- and crust-derived magmas. The striking similarities in the zircon Hf–O isotopic compositions in both MME–host granitoid pairs indicate that the granitoids and MMEs have similar sources. The granitoids are proposed to be mainly sourced from magmas generated by remelting of newly formed mafic rocks, which were generated by earlier basaltic magmas underplating, or injected into, the mid-to-lower crust. The continuing basaltic magma underplating and remelting of earlier-formed mafic rocks in the mid-to-lower crust indicate that the mantle provided both heat and materials for the generation of the Alxa SIP. The scenario also suggests that basaltic magma underplating may play a more important role in the crustal growth in the Alxa SIP than it is generally recognized in other SIPs.

1. Introduction

The generation of large volumes of silicic magmas is commonly accompanied by basaltic magma underplating (Annen and Sparks, 2002; Annen et al., 2006), which provides heat and, potentially, materials for the generation of the felsic magmas. In a silicic large igneous province (SLIP), the fertility of crust plays a crucial role in governing the generation of large volumes of continental silicic magmas (Bryan, 2007; Bryan et al., 2002). Accordingly, underplated basaltic magmas are commonly considered more as a large reservoir of heat rather than a source of silicic magmas (Bryan, 2007; Bryan et al., 2008; Quick et al., 2009; Sinigoi et al., 2011). Nonetheless, some large volumes of silicic magmas are clearly generated by crystal fractionation of primary mantle-derived magmas

* Corresponding authors at: State Key Laboratory of Isotope Geochemistry, Guangzhou Institute of Geochemistry, Chinese Academy of Sciences, Guangzhou, Guangdong 510640, China.
E-mail addresses: danwei@gig.ac.cn (W. Dan), wqiang@gig.ac.cn (Q. Wang).

http://dx.doi.org/10.1016/j.lithos.2015.05.016
0024-4937/

accompanied by some assimilation of local wall-rocks (Deering et al., 2011; Rooney and Deering, 2014). The newly reported 0.05 M km^2 Alxa silicic igneous province (SIP) is composed predominantly of 280 Ma granites (Dan et al., 2014a) and magmatic underplating is confirmed by the coeval basaltic magmas. Interestingly, many mafic microgranular enclaves (MMEs), whose occurrences are not common in SIP, were reported in the granitoids (e.g., Zhang et al., 2012). These MMEs provide an opportunity to study the interaction between mantle-derived mafic and crust-derived felsic magmas in larger SLIPs (>0.1 M km^2: Ernst, 2014).

It is widely accepted that mafic and felsic microgranular enclaves result from the mixing or mingling of mafic and crustal felsic magmas (e.g., Barbarin, 2005; Blundy and Sparks, 1992; Dorais et al., 1990; Feeley et al., 2008; Sun et al., 2010; Vernon, 1984, 1990; Wang et al., 2012; Wiebe et al., 1997; Yang et al., 2006, 2007). Two other proposals suggest that they are: (1) fragments of recrystallized, refractory metamorphic rocks or of melt residues from the granite source (e.g., Chappell and White, 1991; Chappell and Wyborn, 2012; Chappell et al., 1987); or (2) cumulates of early-formed crystals or chilled margins (e.g., Bonin, 1991; Collins et al., 2006; Donaire et al., 2005; Shellnutt et al., 2010; Tindle and Pearce, 1983). Distinguishing between these scenarios requires the ability to characterize the primary source of both the microgranular enclaves and their host granitoids. Compared with whole rock Sr and Nd isotopic compositions, which are easy equilibrated between the microgranular enclaves and adjacent host granitoids (e.g., Barbarin, 2005; Yang et al., 2007), in situ minerals can retain their initial isotopic compositions. Thus, in situ isotopic analysis is commonly used to trace the origin and petrogenetic processes of microgranular enclaves and granites (e.g., Sun et al., 2010).

Zircon, one of the early crystallized minerals and ubiquitous in microgranular enclaves and granites, can be analyzed in situ to determine U–Pb, Hf and O isotopic compositions. The data distinguish the origin and petrogenetic processes of microgranular enclaves and granites (e.g., Sun et al., 2010) because most studies indicate that the MMEs and host granitoids have different zircon Hf and/or O isotope compositions. In this contribution, we present in situ zircon U–Pb age and Hf–O isotopic composition, as well as whole-rock element and Nd–Sr isotopic composition, for two MME–host granitoid pairs in Bayannuoergong batholith and Yamaitu pluton from the Alxa Block. Our work reveals a rare occurrence of similar zircon Hf–O and whole rock Sr–Nd isotopic compositions in the MMEs and their corresponding host granitoids, implying that prolonged basaltic magma underplating and remelting of earlier formed mafic rocks in the mid-to-lower crust play a significant role in the generation of SIPs.

2. Geological setting

The Alxa Block, located in westernmost North China, connects the North China Craton, the Tarim Craton, the Central Asian Orogen Belt (CAOB) and the Qilian Block (Fig. 1a). It has recently been interpreted as an independent block by Dan et al. (2012, 2015), although it was previously thought to be a part of the North China Craton (NCC) (e.g., NMBGMR, 1991; Zhao, 2014; Zhao and Cawood, 2012; Zhao et al., 2005). It is largely covered by desert, and outcrops of pre-Neoproterozoic crystalline basement rocks are only observed in the southwestern parts of the block. The Paleoproterozoic Diebusige and Bayanwulashan complexes (Dan et al., 2012), which were traditionally considered to be part of the eastern Alxa Block, have recently been reinterpreted as part of the NCC (Dan et al., 2015). The oldest rocks are the newly discovered ~2.5 Ga tonalite–trondhjemite–granodiorite (TTG) exposed in the Beidashan Complex (Gong et al., 2012; Zhang et al., 2013) and Paleoproterozoic rocks with ages of ~2.3–1.9 Ga exposed in the Longshoushan Complex that were metamorphosed at ~1.9 Ga and ~1.8 Ga (Gong et al., 2011). The Mesoproterozoic medium- to low-metamorphic grade Alxa Group (Geng et al., 2007) was unconformably covered by Neoproterozoic un-metamorphosed to very low-grade metamorphosed sedimentary sequences (NMBGMR, 1991). In the Neoproterozoic, a few S-type granites with ages of 930–910 Ma intruded in the central Alxa Block (Dan et al., 2014b).

The oldest Phanerozoic sedimentary rocks occur in the Upper Carboniferous–Lower Permian Amushan Formation, mainly in the northern Alxa Block (Fig. 1b). A notable feature of the Alxa Block is that large volumes of Phanerozoic granitoids (NMBGMR, 1991) were formed between 320 Ma and 260 Ma (Fig. 1b) and define a silicic igneous province (Dan et al., 2014a and references therein). Igneous rocks with ages >320 Ma are very rare, apart from a few ~447–394 Ma intermediate-felsic igneous rocks and 345–337 Ma monzogranites in the eastern Alxa Block (Fig. 1b) (Dan et al., 2015; Li, 2006).

3. Geological and rock characteristics of magmatic rocks and MMEs

3.1. Bayannuoergong batholith

The Bayannuoergong batholith was previously described by Dan et al. (2014a). It consists mainly of coarse monzogranites and granodiorites, along with a few diorites and A-type granites and some later felsic dykes (Fig. 2a). MMEs are commonly observed within the monzogranites, especially at pluton margins, and also occur within the granodiorites. The MMEs in the monzogranites range in size from 5 cm to 60 cm and generally appear circular or lenticular in section, with sharp contacts. Locally, MMEs define dyke-like trains (Fig. 3a) that progressively thin toward their terminations within the host granitoids. In some cases, coarse felsic minerals crosscut the enclave/host boundary (Fig. 3b) and some enclaves contain large feldspar megacrysts with corroded cores (Figs. 3b, 4a and b). The MMEs in the granodiorites are commonly 5 cm to 15 cm in size, and show sharp contacts with the host rocks (Fig. 3c). Some enclaves contain large mantled plagioclase megacrysts (Fig. 4d). Apatite is a common accessory mineral in these MMEs, occurring as acicular crystals. The main rock types, including monzogranites and granodiorites and A-type granites, were formed contemporaneously at ~280 Ma (Dan et al., 2014a).

In comparison to their host rocks, the MMEs are fine-grained in texture and monzonitic to dioritic in composition. Both types of MMEs show textures similar to the poikilitic–equigranular textures of basic igneous rocks and do not display any cumulate textures (Fig. 4a–d). The monzonitic enclaves are mainly present in the monzogranites and are composed of plagioclase (35–40 vol.%), alkali feldspar (10–15 vol.%), hornblende (20–30 vol.%), biotite (10–15 vol.%), quartz (10–15 vol.%) and accessory minerals. These assemblages are distinct from those of the host monzogranites and granodiorites, which have hornblende contents of 0–5 vol.% (Dan et al., 2014a). The dioritic enclaves in the granodiorites consist of plagioclase (30–40%), alkali feldspar (5–15 vol.%), quartz (10–20 vol.%), biotite (20–35 vol.%), hornblende (5–10 vol.%) and accessory minerals.

3.2. Yamaitu pluton

The Yamaitu pluton outcrops over about 58 km^2, and intrudes into the Precambrian strata (Fig. 2b). It consists mainly of coarse monzogranites and granodiorites. The MMEs are commonly observed within the granodiorites. They are typically 10 cm to 40 cm in size, and show sharp contacts with the host rocks (Fig. 3d). In contrast to their host rocks, the MMEs are monzonitic in composition, and fine-grained in texture, which is similar to the poikilitic to equigranular textures of basic igneous rocks, and do not demonstrate any cumulate textures (Fig. 4e). Some enclaves contain quartz xenocrysts (Fig. 4e) and acicular apatites are commonly enclosed in plagioclase (Fig. 4f). The granodiorites show myrmekitic texture, and consist of quartz (20–25 vol.%), alkali feldspar (20–30 vol.%), plagioclase (40–50 vol.%), biotite (5–8 vol.%), hornblende (1–2 vol.%) and accessory minerals, including zircon and apatite. The monzonitic enclaves are composed of plagioclase (40–50 vol.%), alkali feldspar (10–20 vol.%), hornblende (20–25 vol.%), biotite (10–20 vol.%), quartz (<5 vol.%) and accessory minerals.

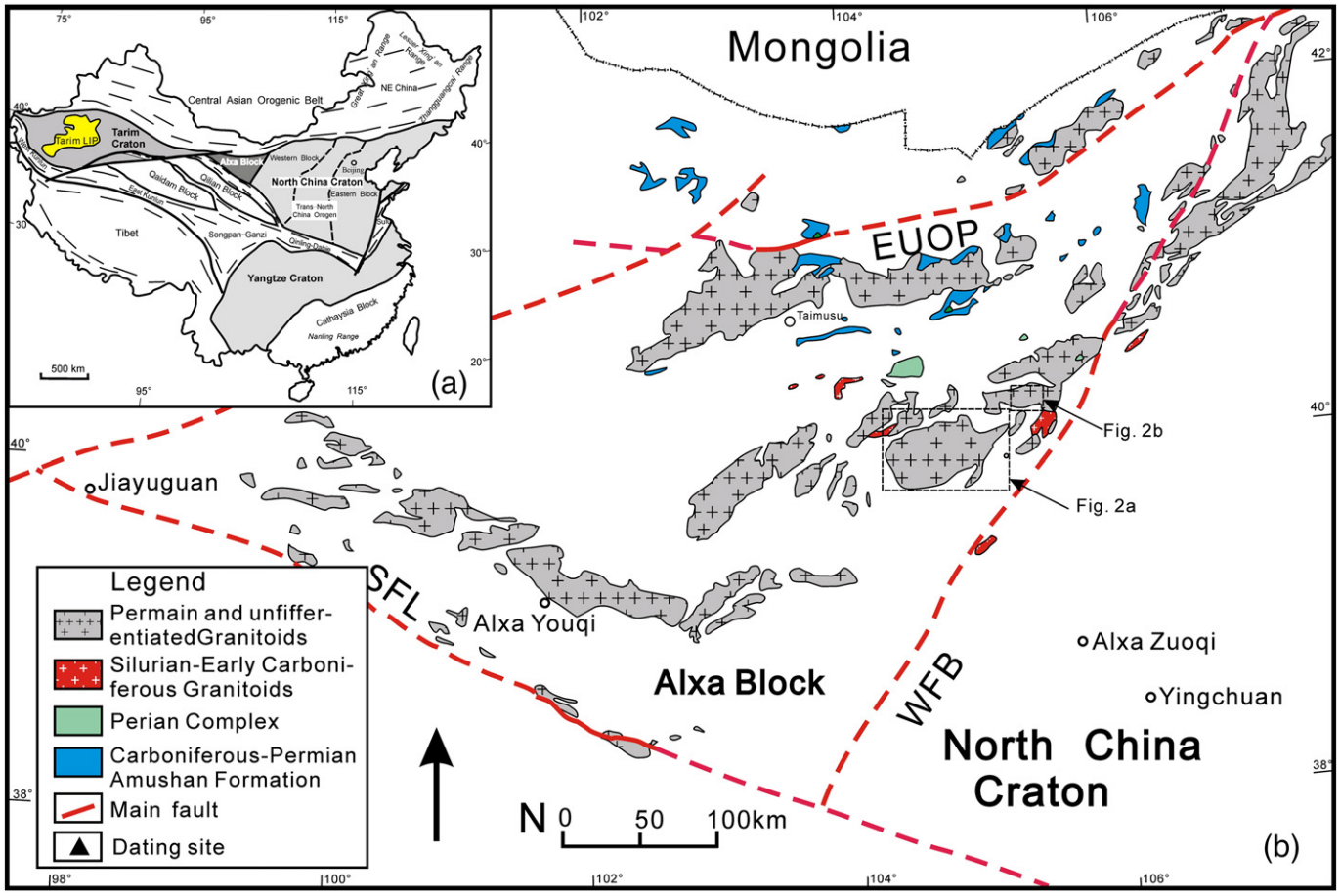

Fig. 1. (a) Tectonic subdivision of China, (b) geological map showing the distribution of Phanerozoic granitoids and Amushan Formation in the Alxa Block and adjacent areas, Tarim LIP, Tarim large igneous province; SFL, southern margin fault of Longshoushan; WFB, western margin fault of Bayanwulashan; EUOB, Enger Us Ophiolite Belt.

4. Analytical procedures

4.1. Zircon U–Pb dating

Isotopic measurements of U, Th and Pb were conducted using the Cameca IMS-1280 SIMS at the Institute of Geology and Geophysics, Chinese Academy of Sciences (IGG-CAS), Beijing, using operating and data processing procedures similar to those described by Li et al. (2009). Uncertainties on individual analyses in the data tables are reported at a 1σ level. Mean ages for pooled U/Pb and Pb/Pb analyses are quoted with 2σ and/or 95% confidence intervals. The weighted mean U–Pb ages and Concordia plots were processed using Isoplot/Ex v.3.0 program (Ludwig, 2003). SIMS zircon U–Pb isotopic data are presented in Supplementary Table A.1.

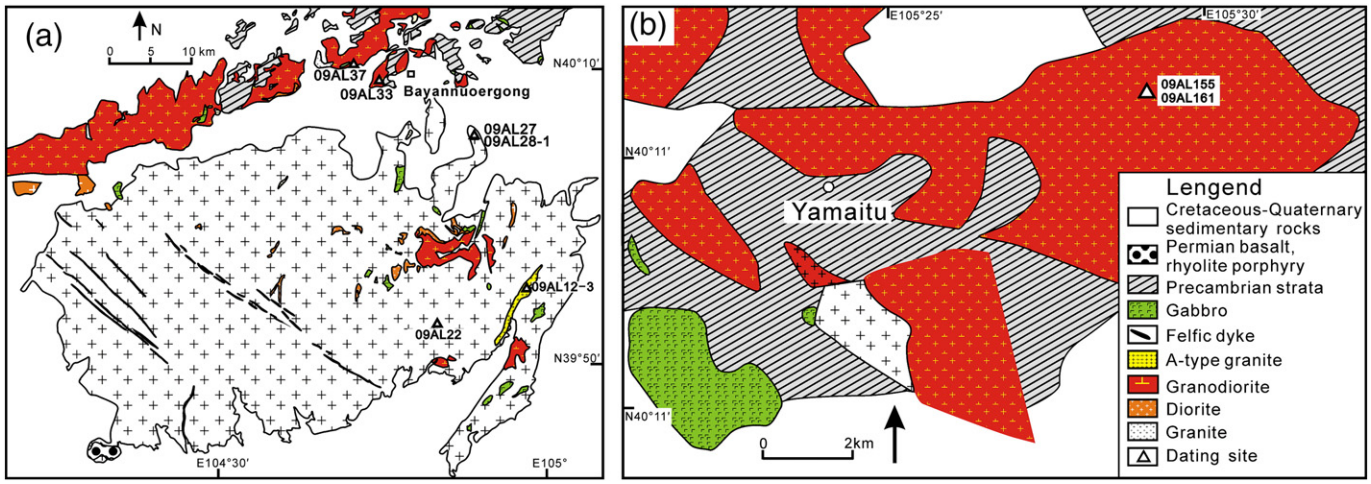

Fig. 2. (a) Geological sketch-map of the Bayannuoergong batholith and (b) Yamaitu pluton, with locations of dating samples.

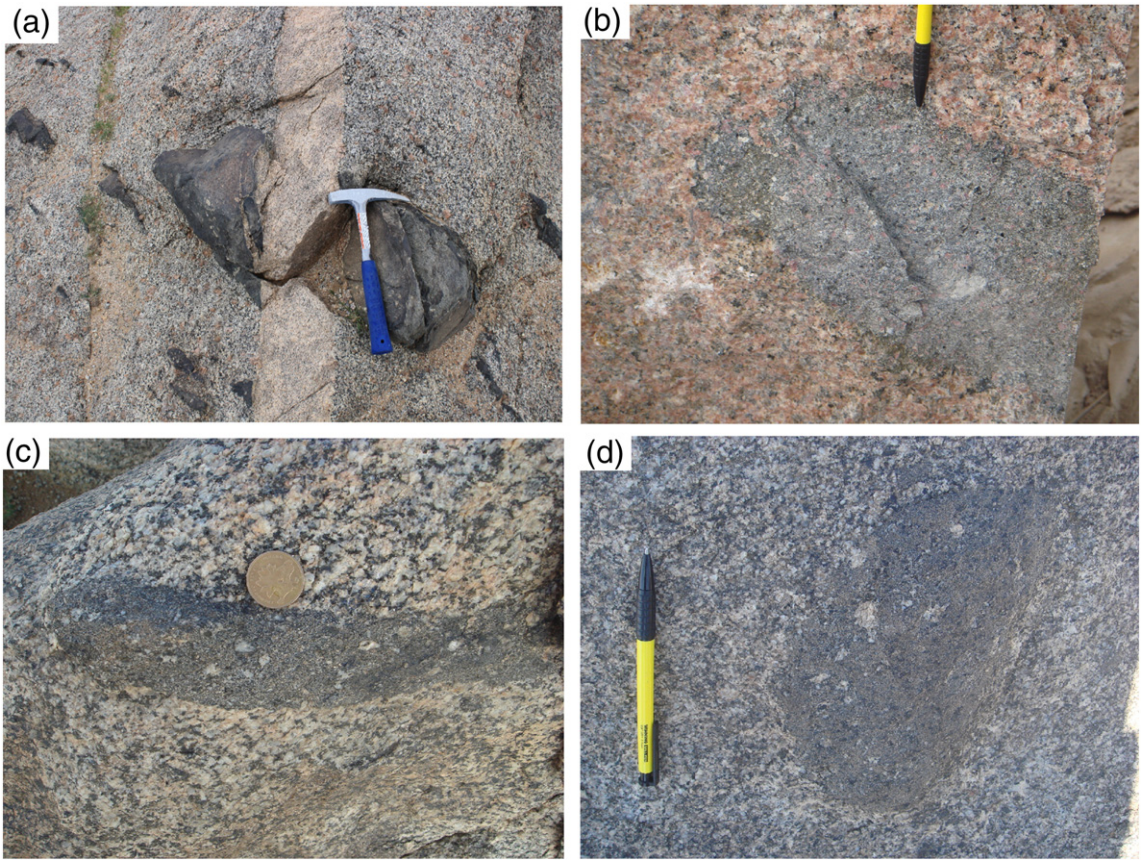

Fig. 3. (a, b) Monzonitic mafic microgranular enclaves (MMEs) occurring within monzogranites and (c) dioritic enclaves within granodiorites in Bayannuoergong batholith, and (d) monzonitic enclaves within granodiorites in Yamaitu pluton.

4.2. Zircon oxygen isotopes

Zircon oxygen isotopes were measured using the same Cameca IMS-1280 SIMS at IGG-CAS. The detailed analytical procedures were similar to those described by Li et al. (2010a). The measured oxygen isotopic data were corrected for instrumental mass fractionation (IMF) using the Penglai zircon standard ($\delta^{18}O_{VSMOW} = 5.3‰$) (Li et al., 2010b). The internal precision of a single analysis generally was better than 0.2‰ (1σ standard error) for the $^{18}O/^{16}O$ ratio. The external precision, measured by the reproducibility of repeated analyses of Penglai standard, is 0.41‰ (2SD, n = 120). Ten measurements of the 91500 zircon standard during the course of this study yielded a weighted mean of $\delta^{18}O = 10.2 \pm 0.5‰$ (2SD), which is consistent within errors with the reported value of 9.9 ± 0.3‰ (Wiedenbeck et al., 2004). Zircon oxygen isotopic data are listed in Supplementary Table A.2.

4.3. Zircon Lu–Hf isotopes

In situ zircon Lu–Hf isotopic analyses were carried out on a Neptune multi-collector ICP-MS equipped with a Geolas-193 Geolas 2005 excimer ArF laser ablation system at the State Key Laboratory of Geological Processes and Mineral Resources, China University of Geosciences in Wuhan. Lu–Hf isotopic analyses were conducted on the same zircon grains that were previously analyzed for U–Pb and O isotopes. Detailed analytical procedures were similar to those described by Hu et al. (2012). Measured $^{176}Hf/^{177}Hf$ ratios were normalized to $^{179}Hf/^{177}Hf = 0.7325$. Further external adjustment was not applied for the unknowns because our determined $^{176}Hf/^{177}Hf$ ratios for zircon standards 91500 (0.282308 ± 0.000004) and GJ-1 (0.282021 ± 0.000011) were in good agreement within errors with the reported values (Griffin et al., 2006; Wu et al., 2006; Zeh et al., 2007). Zircon Hf isotopic data are listed in Supplementary Table A.2.

4.4. Major and trace elements

Twenty-one powdered rock samples of ~200-mesh size were used for geochemical analyses. Major element oxides were analyzed on fused glass beads using a Rigaku RIX 2000 X-ray fluorescence spectrometer at the State Key Laboratory of Isotope Geochemistry, the Guangzhou Institute of Geochemistry, Chinese Academy of Sciences (SKLaBIG GIG CAS). Calibration lines used in quantification were produced by bivariate regression of data from 36 reference materials encompassing a wide range of silicate compositions (Li et al., 2005). Analytical uncertainties are between 1% and 5%. Trace elements were analyzed using an Agilent 7500a ICP-MS at GIG-CAS. Analytical procedures were similar to those described by Li et al. (2000). A set of USGS and Chinese national rock standards, including BHVO-2, GSR-1, GSR-2, GSR-3, AGV-2, W-2 and SARM-4, was chosen for calibration. Analytical precision is typically better than 5%. Geochemical results are listed in Supplementary Table A.3.

4.5. Sr and Nd isotopic compositions

Whole rock Rb–Sr and Sm–Nd isotopic analyses (Supplementary Table A.4) were also determined for the 16 samples. Sr–Nd isotopic compositions were determined using a Micromass Isoprobe multi-collector ICP-MS at SKLaBIG GIG CAS, and analytical procedures described by Li et al. (2004). Sr and Nd were separated using cation columns, and Nd fractions were further separated by HDEHP-coated Kef columns. The measured $^{87}Sr/^{86}Sr$ ratio of the NBS 987 standard and $^{143}Nd/^{144}Nd$ ratio of the JNdi-1 standard were 0.710274 ± 18 (n = 11, 2σ) and 0.512093 ± 11 (n = 11, 2σ), respectively. All measured

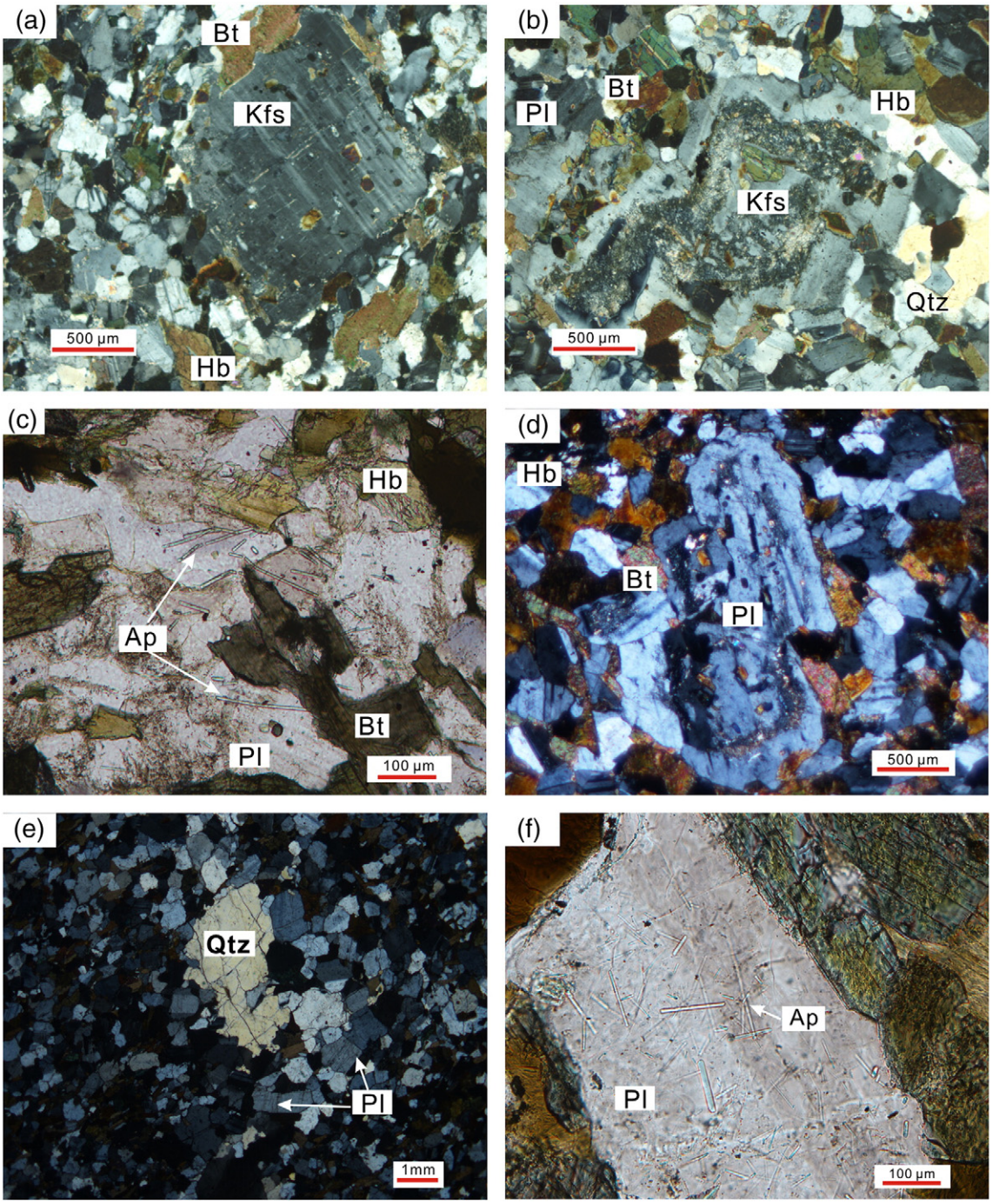

Fig. 4. Bayannuoergong batholith: (a, b) large K-feldspar grain and (c) acicular apatites in monzonitic enclaves and (d) large plagioclase grain in dioritic enclave; Yamaitu pluton: (e) xenocrystic quartz with plagioclase and (f) acicular apatites in monzonitic enclaves.

Nd and Sr isotope ratios were normalized to $^{146}Nd/^{144}Nd = 0.7219$ and $^{86}Sr/^{88}Sr = 0.1194$, respectively.

5. Results

5.1. Zircon U–Pb dating results

Zircon grains separated for dating are mostly euhedral to subhedral, with length of ~100–150 μm, and length to width ratio of 2:1 to 4:1. The zircon grains in both MMEs and host granitoids show similar oscillatory zoning CL images, and have high Th/U ratios (0.26–0.92) (Supplementary Table A.1) that suggest magmatic origins (Belousova et al., 2002). It is noted that the MMEs have lower Th contents and Th/U ratios, compared to their host granitoids (Fig. 5d). U–Pb Concordia diagrams of analyzed zircons are shown in Fig. 5, and the U–Pb age data are given in Supplementary Table A.1.

For the Bayannuoergong batholith, a monzonitic enclave (09AL28-1) was selected for U–Pb dating, and it gave a weighted mean $^{206}Pb/^{238}U$ age of 278 ± 2 Ma (MSWD = 0.68, n = 12) (Fig. 4a). This age is similar to the ages (284–278 Ma) of host granitoids and granodiorites (Dan et al., 2014a). For the Yamaitu pluton, the host granodiorite (09AL155) and enclave (09AL161) samples gave weighted mean $^{206}Pb/^{238}U$ ages of 270 ± 2 Ma (Fig. 4b) and 272 ± 2 Ma (Fig. 4c), respectively. In summary, the zircon U–Pb age data indicate that there are two stages of MME generation, which are coeval with their host granitoids.

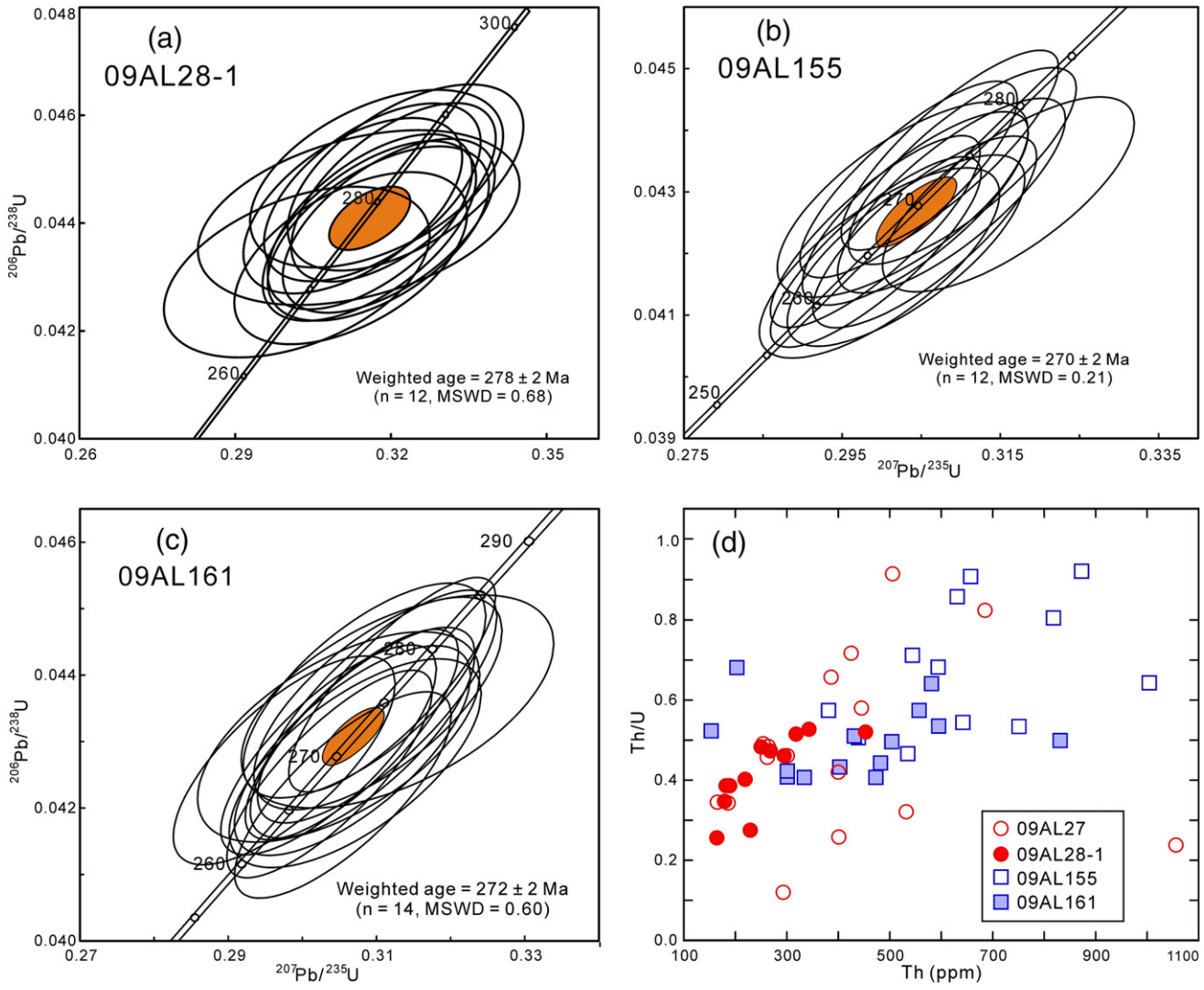

Fig. 5. SIMS U–Pb Concordia diagrams for the MMEs and host granitoids in Alxa Block. (a) Monzonitic enclave from Bayannuoergong batholith (09AL28-1), (b) granodiorite and (c) monzonitic enclave from Yamaitu pluton. Data-point error ellipses are 2σ. (d) Th vs. Th/U for zircon from MMEs and host granitoids.
The data for sample 09AL27 are from Dan et al. (2014a).

5.2. Whole-rock major and trace element compositions

Samples from both Yamaitu pluton and Bayannuoergong batholith exhibit broad compositional variation, with SiO_2 ranging from 50.7 to 61.4 wt.% (volatile free) in MMEs and from 63.6 to 77.5 wt.% (volatile free) in host granitoids (Fig. 6, Supplementary Table A.3). The MMEs have relatively higher MgO (2.6–4.9 wt.%), Cr (23–146 ppm) and Ni (6–38 ppm), but relatively lower Th (0.8–2.8 ppm) contents than those (MgO (0.23–2.1 wt.%), Cr (10–38 ppm), Ni (5–14 ppm) and Th (5.2–41 ppm)) of the host granitoids (Supplementary Table A.3) (Fig. 7). On Harker diagrams, granodiorites and MMEs define broadly linear trends (Fig. 7). However, these geochemical features of the MMEs and host granitoids cannot be used to identify their sources and the magmatic process involved, since both fractionation and magma mixing can lead to such a linear trend (Sun et al., 2010).

Chondrite-normalized rare earth element (REE) patterns and primitive mantle-normalized trace element spidergrams are presented in Fig. 8. Both MMEs and host rocks have high total REE contents and show REE fractionation with relative enrichment of light REEs. The monzonitic enclaves show less fractionation in the REEs (La_N/Yb_N = 2–4) than in the host granitoids (La_N/Yb_N = 3–48), and the monzonitic enclaves have relatively high abundances of REEs (especially heavy REEs), which result in flatter normalized patterns when compared with the granitoids (Fig. 8a and c). Another noticeable feature of the MMEs is the convex distribution pattern of their light REEs, resulting in a low $(La/Ce)_N$ ratio (0.87–1.03). In contrast to the low $(La/Yb)_N$ ratios (2–4) and negative Eu anomalies in monzonitic enclaves from both Yamaitu pluton and Bayannuoergong batholith, the two dioritic enclaves from Bayannuoergong batholith have high $(La/Yb)_N$ ratios (5–9) with no Eu anomalies, similar to their host granodiorites. On primitive mantle-normalized incompatible element diagrams (Fig. 8b, d), both granitoid and MME samples show Nb–Ta troughs, but to varying extents. The MMEs exhibit a relatively high degree of variation in Th concentrations. The monzonitic enclaves show negative anomalies in Sr, Eu and Zr, whereas the dioritic enclaves show positive anomalies in Ba, Sr and Eu. The dioritic enclaves are also characterized by relatively high Sr (454–507 ppm) but low Yb (≤1.5 ppm) and Y (≤14 ppm) contents with high Sr/Y ratios of 31–38, similar to the host granodiorites (Dan et al., 2014a).

5.3. Whole rock Sr–Nd isotopic compositions

For ease of comparison, the initial Rb–Sr and Sm–Nd isotopic compositions of all 16 samples are calculated at 270 Ma, although enclaves from the Bayannuoergong batholith are dated at 278 Ma (Supplementary Table A.4) (Fig. 9). In the Yamaitu pluton, both enclaves and granodiorites

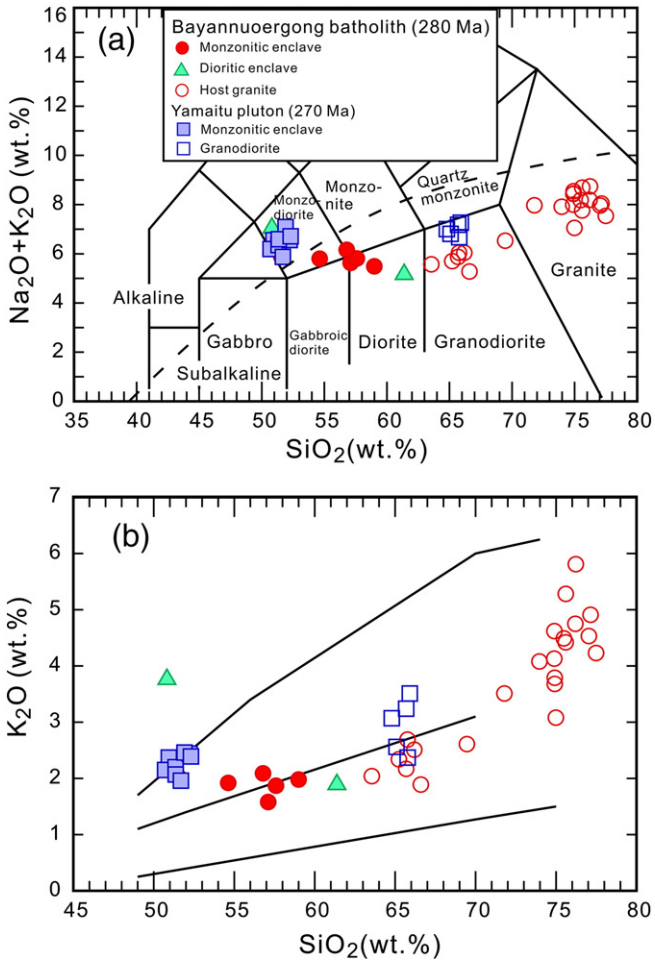

Fig. 6. (a) SiO_2 vs. $K_2O + Na_2O$ diagram for intrusive rocks (Middlemost, 1994), (b) SiO_2 vs. K_2O diagram (Peccerillo and Taylor, 1976). The granites in Bayannuoergong batholith (Dan et al., 2014a) are shown in this figure and Figs. 7–10.

have almost identical initial $^{87}Sr/^{86}Sr$ isotopic ratios (I_{Sr}), ranging from 0.7068 to 0.7070 and from 0.7067 to 0.7072, respectively (Supplementary Table A.4). Six mafic enclave samples have identical $\varepsilon_{Nd}(t)$ values ranging from −11.9 to −11.3, similar to those (−12.8 to −11.5) of the host granodiorites. Isotopic analysis of one host granitoid sample (09AL155) immediately adjacent to the mafic enclaves yielded $I_{Sr} = 0.7071$ and $\varepsilon_{Nd}(t) = -11.5$, within the range of whole-rock enclave compositions.

In the Bayannuoergong batholith, both monzonitic and dioritic enclaves have similar initial $^{87}Sr/^{86}Sr$ isotopic ratios of 0.7090–0.7095 and similar $\varepsilon_{Nd}(t)$ values of −14.7 to −13.2 (Supplementary Table A.4). The host monzogranites have initial $^{87}Sr/^{86}Sr$ isotopic ratios ranging from 0.7064 to 0.7094 and $\varepsilon_{Nd}(t)$ values ranging from −13.3 to −9.7 (Supplementary Table A.4; Dan et al., 2014a). The mafic enclaves have similar Sr–Nd isotopes with their adjacent host granitoids, such as pairs of 09AL30 (mafic enclave) and 09AL29 (host monzogranite), and 09AL38 (mafic enclave) and 09AL40 (host granodiorite) (Fig. 9).

5.4. Zircon Hf–O isotopic compositions

In situ LA-MC-ICP-MS Lu–Hf isotopic analyses were conducted on the zircon grains that were previously analyzed for U–Pb and/or O isotopes. Their results are presented in Supplementary Table A.2 and Fig. 10. Zircons from one enclave sample (09AL28-1) have a small range of initial $^{176}Hf/^{177}Hf$ isotopic ratios of 0.282180–0.282328, corresponding to $\varepsilon_{Hf}(t)$ values of −14.8 to −9.6, similar to those (−14.5 to −7.5, one is −20.0) of the adjacent host granite (09AL27). Zircons from samples 09AL155 to 09AL161 have similar initial $^{176}Hf/^{177}Hf$ isotopic ratios of 0.282280–0.282359 and 0.282287–0.282359, corresponding to $\varepsilon_{Hf}(t)$ values of −11.5 to −8.7 and −11.2 to −8.6, respectively. The measured $\delta^{18}O$ values for zircons from 09AL28-1 (monzonitic enclave), 09AL155 and 09AL161 show limited ranges of 5.9–6.8‰, 5.1–6.2‰ and 5.1–5.9‰, forming normal Gaussian distributions, with averaged values of 6.30 ± 0.23‰ (1SD), 5.61 ± 0.30‰ (1SD) and 5.59 ± 0.22‰ (1SD), respectively.

It is noted that each MME–host granitoid pair has similar zircon Hf–O isotopes. In the Yamaitu pluton, zircon Hf–O isotopes of the enclave (09AL161) are almost identical to those of the host granite (09AL155) (Fig. 10). In the Bayannuoergong batholith, the monzonitic enclave (09AL28-1) also has similar zircon Hf–O isotope compositions to the adjacent host granite (09AL27) (Fig. 10). The slight difference between them implies that the host granite is contaminated by ^{18}O-depleted rocks and Precambrian materials (Dan et al., 2014a). The contamination is also reflected in the whole rock Sr–Nd isotopes, as the enclave (09AL28-1) has more depleted isotopes than the adjacent host granite (09AL27) (Fig. 9a).

6. Discussion

6.1. Magma mixing for generating the mafic microgranular enclaves

As previously noted, there are many interpretations regarding the origin of microgranular enclaves, including residues after partial melting, cumulates formed by early crystallization, or magma mixing. The restite model is mostly applied to S-type granites where the microgranular enclaves have a metamorphic or residual sedimentary fabric (Chappell et al., 1987; White et al., 1999). A critical feature of the restite model is linear chemical variations, which are observed in many calc-alkaline plutonic suites (e.g., Chappell and White, 1991; Chappell et al., 1987; Collins, 1998). However, these features (Fig. 7) can also be attributed to crystallization fractionation or magma mixing, and some elements such as Al_2O_3 and MgO show different trends between the MMEs and host granitoids. Moreover, the enclave textures are igneous not metamorphic (e.g., Vernon, 1984), and abundant magmatic biotites and acicular apatites in the studied MMEs also argue against the restite model (Vernon, 2007). Thus, only the latter two models were considered in detail for the generation of the two types of MMEs in the Alxa Block granites.

The similar mineral assemblages and isotopic compositions of the MMEs and host granitoids in both plutons, which are considered further in Section 6.2, are commonly used to indicate that the microgranular enclaves crystallized from coeval, cognate host magmas via accumulation (Dahlquist, 2002; Dodge and Kistler, 1990) or chilled margins processes (Donaire et al., 2005; Esna-Ashari et al., 2011; Pascual et al., 2008). The cumulate model has been criticized because it would not be compatible with the small grain size and the fine-grained margins of many enclaves (Donaire et al., 2005; Esna-Ashari et al., 2011). In the chilled margin scenario, microgranular enclaves have high SiO_2 contents (commonly >58 wt.%) (Donaire et al., 2005; Esna-Ashari et al., 2011; Pascual et al., 2008), can be classified as intermediate-felsic microgranular enclaves (Didier and Barbarin, 1991) and the major mafic mineral is biotite (Donaire et al., 2005; Esna-Ashari et al., 2011; Pascual et al., 2008). These characteristics are not observed in the studied MMEs. All of the studied enclaves are fine grained mafic enclaves, all but two have SiO_2 contents <58 wt.% (Fig. 6a), and their major mafic minerals are amphibole, which is reflected in their low $(La/Ce)_N$ ratios (Fig. 8a, c) (Dorais et al., 1990; Tang et al., 2012; Zi et al., 2012).

The following lines of evidence suggest mixing between mantle-derived mafic and crust-derived felsic magmas for the origin of both types of MMEs. The abundant acicular apatite and the pervasive poikilitic texture of enclaves (Fig. 4) support the interpretation of rapid crystallization of a basaltic magma brought into close proximity to cooler partially crystallized felsic magma. The apatite occurring as acicular crystals is also suggestive of a magma mixing origin (Hibbard,

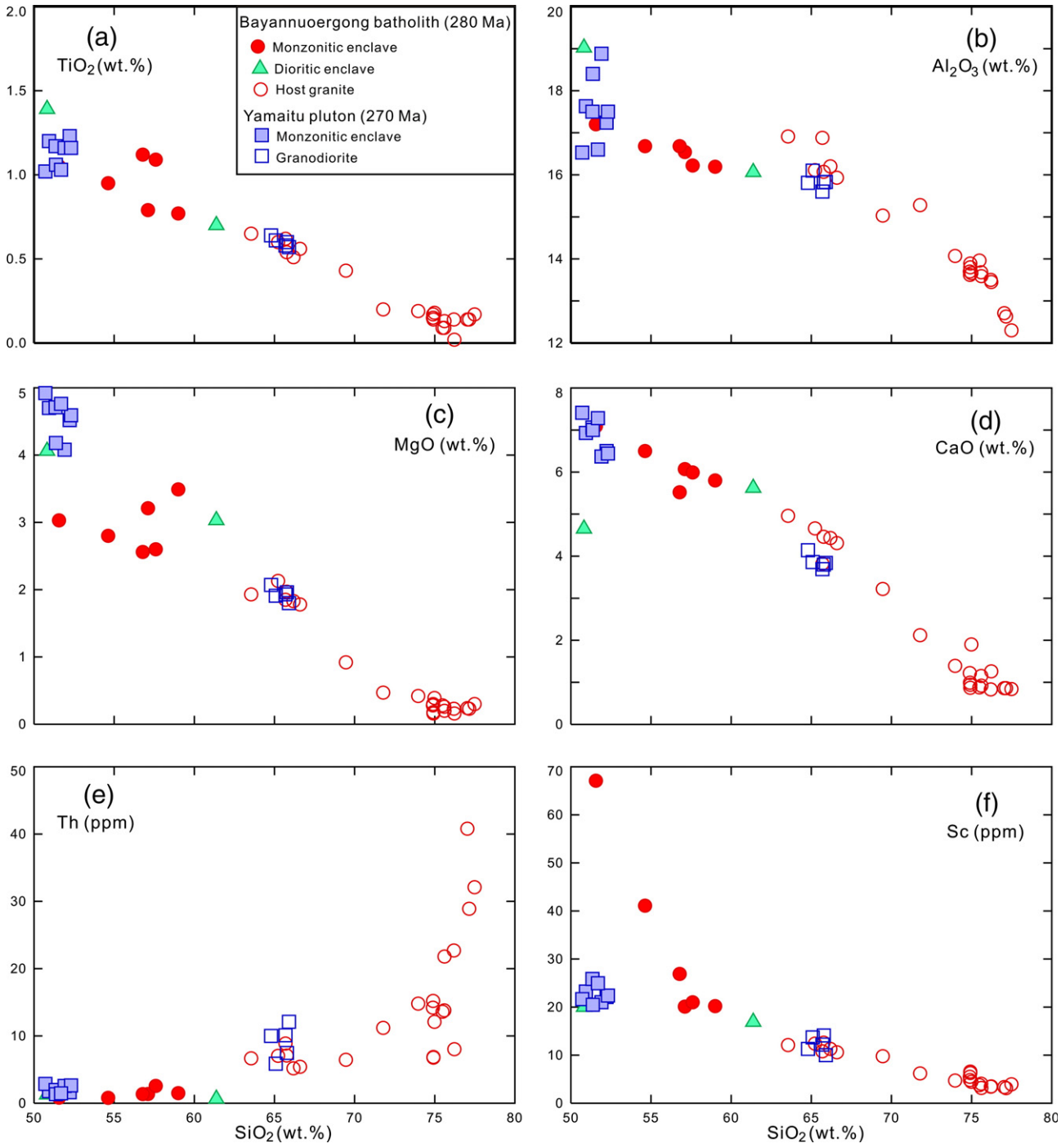

Fig. 7. Selected major oxide (wt.%) and trace elements (ppm) vs. SiO_2 (wt.%) for the MMEs and host granitoids.

1991). The enclaves have igneous microtextures and textural evidence for disequilibrium, such as plagioclase and K-feldspar with complex oscillatory zoning and repeated resorption surfaces and quartz xenocryst (Fig. 4b, d, e), which are analogous to other cases of magma mixing from around the world (e.g., Bonin, 2004; Didier and Barbarin, 1991; Vernon, 1984, 2007). Furthermore, although the host granitoids show a wide range of isotopic compositions (Fig. 7a), the MMEs have isotopic compositions similar to their adjacent host granitoids. This scenario is an analogy to the well-known examples of mixing of mafic and felsic magmas suggested for the origin of MMEs, as enclave abundance increases, the host composition shifts toward the enclave composition (e.g. Silva et al., 2000). In summary, the occurrences of quartz xenocrysts, K-feldspar megacrysts, corroded feldspars and acicular apatites are consistent with the interpretation that the MMEs are the products of magma mixing.

It is noted that the dioritic enclaves show geochemical characteristics different from the monzonitic enclaves (Fig. 8). However, the dioritic and monzonitic enclaves have Nd–Sr–O isotope compositions similar to their host granodiorites and monzogranites or granodiorites, respectively (Figs. 8–10). Thus, the generation of the two types of enclaves must be similar to their corresponding host granitoids. Dan et al. (2014a) proposed that the granodiorites and monzogranites of the Bayannuoergong batholith were generated in thickened and normal crust, respectively. Accordingly, the corresponding depths for generation of the dioritic enclaves were deeper than those of the monzonitic enclaves.

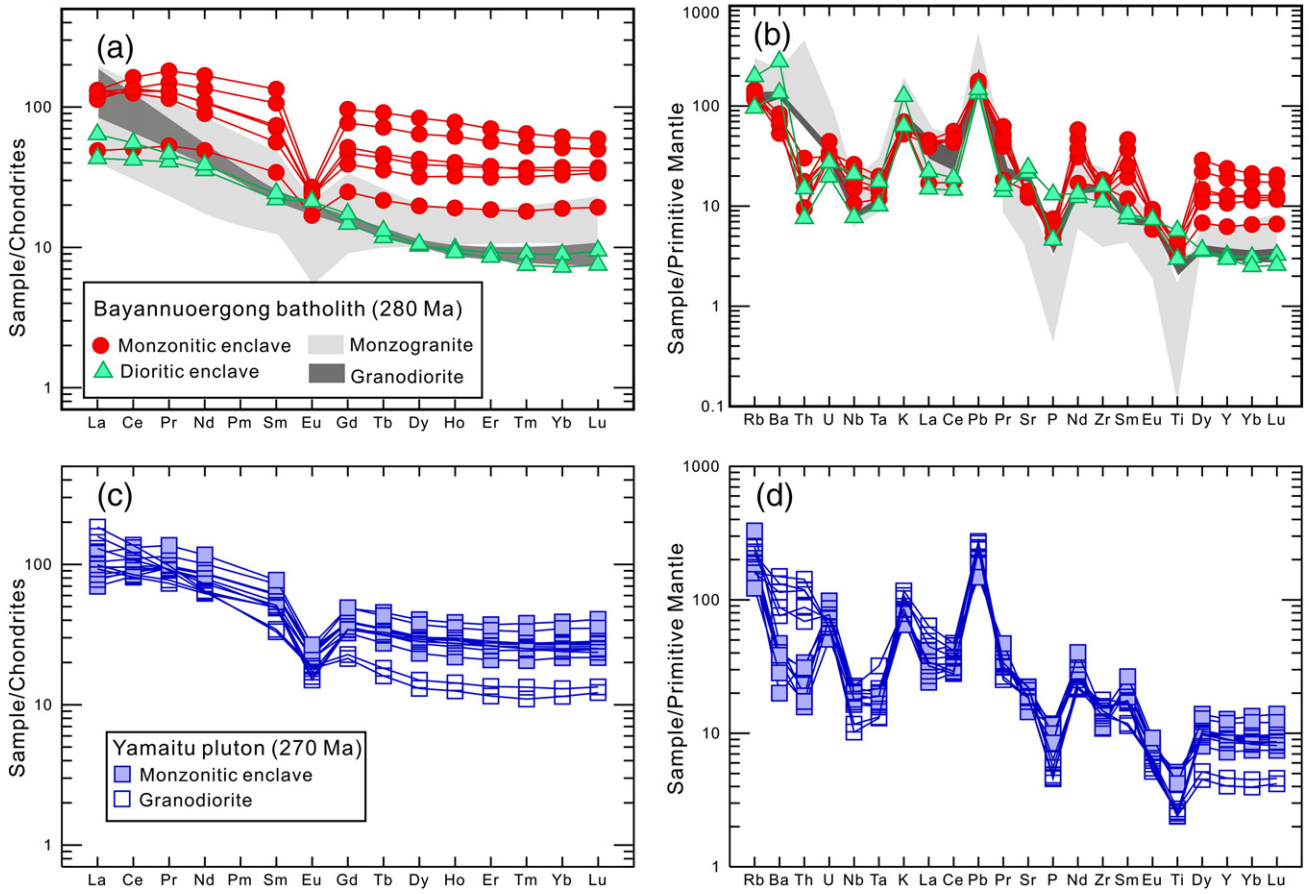

Fig. 8. (a, c) Chondrite-normalized REE diagrams and (b, d) primitive mantle- normalized incompatible trace element spidergrams for the MMEs and host granitoids. The normalization values are from Sun and McDonough (1989).

6.2. Implications of similar MME and host granitoid isotopic compositions

By themselves, the petrographic features of the MMEs appear consistent with a common magma mixing scenario. The compositional similarities in whole rock Sr–Nd and zircon Hf–O isotopic characteristics of the enclaves and host granitoids (Figs. 9 and 10), however, require a more detailed explanation, particularly since the two MME–host granitoid pairs belong to two stages of magma generations with different Sr–Nd–Hf–O isotopic signatures.

The two sets of similar signatures, particularly the zircon Hf–O isotopes, could be the result of one of three processes: (1) zircon grains in the MMEs were transported from the host granitoids during magma mixing, (2) the MMEs and host granitoids attained isotopic equilibration during magma mingling and mixing (e.g., Allen, 1991; Barbarin, 2005; Dorais et al., 1990; Eberz and Nicholls 1990; Tindle, 1991) and (3) the mafic and felsic magmas had similar isotopic compositions (Zi et al., 2012). Although the introduction of crystals, such as K-feldspars, from host to enclave magmas has been documented in this study

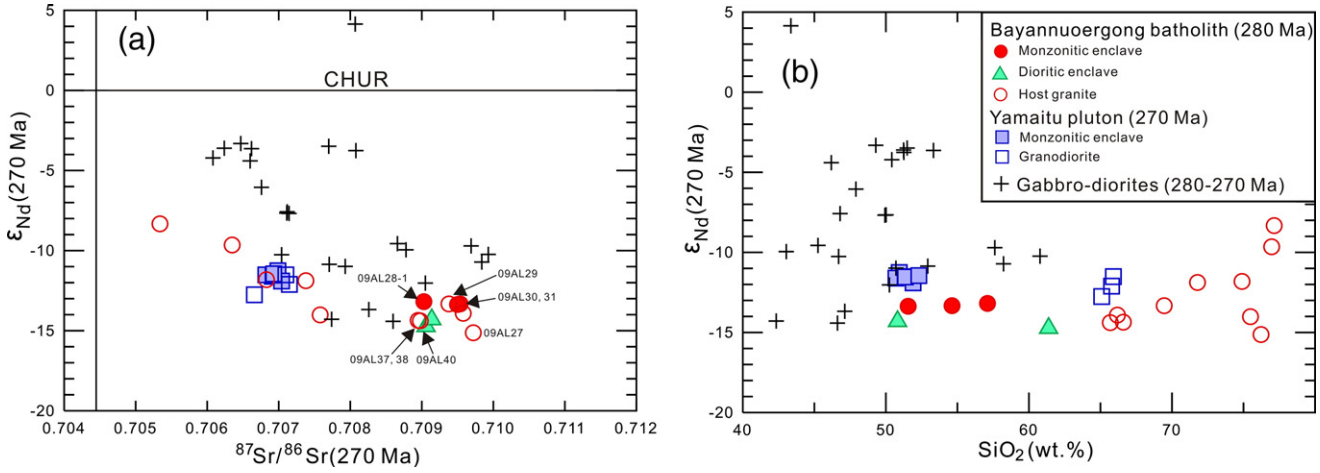

Fig. 9. (a) Nd–Sr isotope composition, (b) $\varepsilon_{Nd}(t)$ values vs. SiO_2 for the MMEs and host granitoids. The 280–270 Ma gabbro-diorites data are from Dan et al., 2014a (submitted for publication).

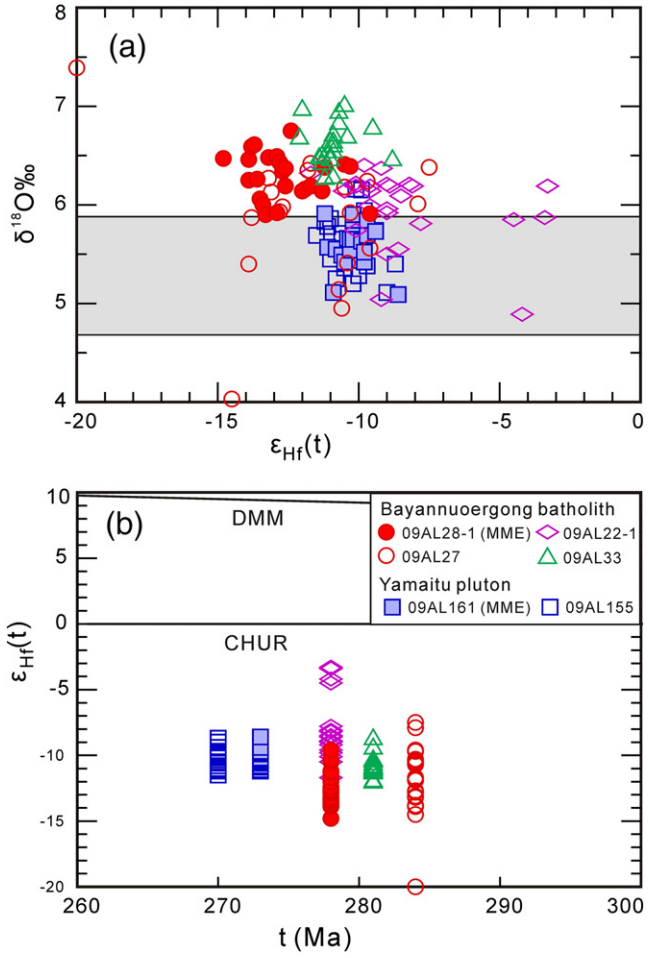

Fig. 10. Plots of (a) $\varepsilon_{Hf}(t)$ values vs. $\delta^{18}O$ values and (b) $\varepsilon_{Hf}(t)$ values vs. crystallization ages for the magmatic zircons from the Early Permian rocks. The shaded field depicts the $\delta^{18}O$ value (5.3 ± 0.6‰, 2SD) of the mantle–derived zircons (Valley et al., 1998).

(Fig. 4a, b), zircons from the MMEs have lower Th contents and Th/U ratios than those of the granites (Fig. 5d), which excludes the first scenario. Whole rock isotopic equilibration between MMEs and host granitoids is common during magma mixing and magma crystallization, especially for the Sr isotopes (e.g., Allen, 1991; Holden et al., 1991; Lesher, 1990). Although the host granitoids show variation in Sr and Nd isotopic compositions, there are similarities between the MMEs and adjacent host granitoids. This scenario could indicate the isotopic equilibration between MMEs and host granitoids. However, the zircon grains, commonly included in other minerals (Bea, 1996), typically retain their original isotopic compositions, suggesting that the MMEs and host granitoids should have different zircon Hf and/or O isotopes if their original magmas had different isotopic signatures (e.g., Griffin et al., 2002; Liu et al., 2013; Sun et al., 2010; Yang et al., 2007). For example, even cryptic mixing can be revealed by in situ zircon Hf–O isotopes (Appleby et al., 2008; Dan et al., 2014c; Kemp et al., 2007). Accordingly, the similar zircon Hf and O isotopic compositions of the MMEs and host granitoids in this study most likely reflect the fact that the mafic and felsic magmas have similar compositions, although a role for local isotopic equilibration cannot be excluded.

The occurrence of similar whole rock and in situ zircon isotopic compositions between mafic and felsic magmas is not unique in cases of mafic–felsic magmas interaction (e.g., Zi et al., 2012). The MMEs could represent a mantle-derived mafic component that replenished the magma chamber and which survived mixing with the evolved host magma (Zi et al., 2012). In this process, minerals display similar crystal sizes for both main and accessory phases, and only weak quenching boundaries are observed (Zi et al., 2012). The occurrences of quartz xenocrysts, K-feldspar and plagioclase megacrysts and acicular apatites in this study do not favor this possibility. Felsic magmas can also acquire isotopic compositions similar to associated basaltic magmas if they are generated by partial remelting of earlier, but related, basaltic magma underplated in the mid-to-lower crust. The time interval between the underplating and partial remelting is not long, thus the isotopic compositions remain nearly the same. Mafic rocks with ages of 280–270 Ma, contemporaneous with the felsic magma generation, are widespread in the Alxa Block, although their volume is small (Dan et al., 2014a). Some of these occurrences have Sr–Nd isotopic signatures similar to the MMEs and granites (Fig. 9). Therefore, we propose that major components of the Yamaitu pluton and Bayannuoergong batholith were sourced from magmas generated by partial remelting of earlier underplated mafic rocks (Fig. 11), which then mixed with later intrusions of related basaltic magmas.

Another distinctive feature of the two MME generations is that the 280 MMEs (Bayannuoergong) have lower whole rock $\varepsilon_{Nd}(t)$ and higher initial $^{87}Sr/^{86}Sr$ values and zircon $\delta^{18}O$ values than those of the 270 MMEs (Yamaitu) (Figs. 9 and 10). Given that published and unpublished data (Dan et al., 2014a, 2015) consistently demonstrate low whole rock $\varepsilon_{Nd}(t)$ values (Fig. 9) for the 280–270 Ma mafic rocks and MMEs, they were probably sourced from the lithospheric mantle. Thus, the simplest and most plausible explanation is that the lithospheric mantle in the Alxa Block is locally heterogeneous, both in radioactive (Sr and Nd) and stable isotopes (O). The 270 Ma MMEs have low zircon $\delta^{18}O$ values 5.59 ± 0.22‰, only slightly higher than the depleted mantle values of 5.3 ± 0.3‰ (Valley et al., 1998), indicating that their source region in the lithospheric mantle underwent only low degrees of fluid metasomatism. This suggestion is supported by the fluid–mobile trace element ratios, such as Ba/Th, which can be used to gauge the extent of fluid enrichment (Hawkesworth et al., 1997). The lower Ba/Th values (49–203) of the 270 Ma enclaves compared with those (212–566 and 1529–1467) of the 280 Ma examples are consistent with lower degrees of fluid metasomatism in the younger MMEs.

6.3. Large mantle component inputs in generation of the silicic igneous province

The generation of Phanerozoic SLIPs is generally ascribed to partial melting of the fertile, hydrous lower-crustal materials, which is triggered by the large-scale and sustained mantle thermal and material inputs into the crust (e.g., Bryan and Ferrari, 2013; Bryan et al., 2002; Ernst, 2014). As discussed above, however, the similar isotopic compositions of two-stage Alxa MMEs and host granitoids suggest that the underplated mafic rocks underwent remelting due to later basaltic magma intrusion. MMEs have also been discovered in other Alxa plutons that have Sr and Nd isotope compositions similar to the

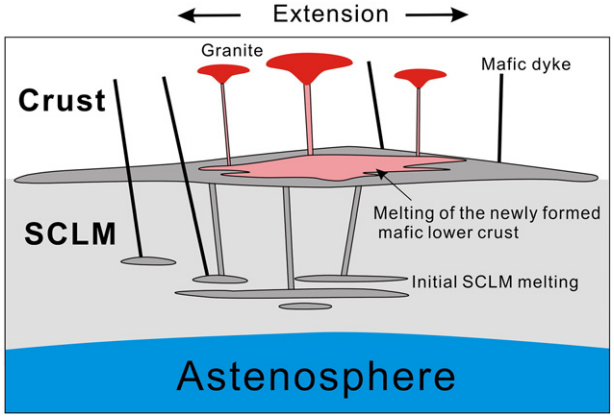

Fig. 11. The model for generating the Permian granitoids in the Alxa Block.

Bayannuoergong batholith and Yamaitu pluton (our unpublished data). This suggests that the scenario outlined here is probably not restricted to these two plutons but prevails throughout the entire evolution of the Alxa SIP. Accordingly, the felsic rocks were not mainly generated by the remelting of reworked ancient lower crust but instead by the widespread remelting of mafic rocks newly formed by basaltic magma underplating or injection into the mid-to-lower crust.

A similar process has been proposed by Annen et al. (2006) and may occur in many tectonic settings, such as subduction zones or rifts. Studies reporting the generation of related felsic magmas (Atherton and Petford, 1993; Petford and Atherton, 1996) are comparatively rare, although basaltic magma underplating (Annen et al., 2006; Li et al., 2014; Petford and Gallagher, 2001) and partial melting of normal (Bryan et al., 2002) or thickened mafic lower crust (Chung et al., 2003; Johnson et al., 1997; Wang et al., 2005, 2006a,b) have been documented in many cases. The difficulties in identifying magmas sourced from such newly-formed mafic rocks likely occur because the volumes of magma are relatively small in volume and may be masked by the predominance of ancient crust-derived magmas or mantle-derived magmas, and/or due to the lack of isotopic contrast between the mantle and the new crustal sources (Frost et al., 2001). The recognition of similar zircon and whole rock isotopic compositions in MMEs and host granitoids provides another way to recognize the remelting of newly-formed mafic rocks in the mid-to-lower crust, in addition to evidence of similar isotopic compositions between the contemporaneous mantle-derived and crustal-derived rocks (Borg and Clynne, 1998; Neves et al., 2000; Zhao et al., 2013), and depleted isotopic compositions of granitoids (Jahn et al., 2000). The technique can be applied in the absence of exposed contemporaneous mafic suites and provides more direct evidence of mantle isotopic properties than given by granitoid data alone.

Continuing basaltic magma underplating and remelting of earlier formed mafic rocks in the mid-to-lower crust imply that substantial crustal growth occurred with generation of the Alxa SIP. It is noted that almost all the Nd isotopic compositions from granitoids are unradiogenic and $\varepsilon_{Nd}(t)$ values are negative in the Alxa SIP (Dan et al., 2014a and this study), unlike the prevalent positive $\varepsilon_{Nd}(t)$ values or zircon $\varepsilon_{Hf}(t)$ from typical granitoids of other crustal growth settings, such as accretionary orogens (CAOB, Jahn et al., 2000; Sengör et al., 1993) and mafic large igneous provinces (Emeishan, Xu et al., 2008; Zhong et al., 2011). The reason is that the underplated mafic rocks in the mid-to-lower crust are mostly generated by partial melting of ancient metasomatized lithospheric mantle in the Alxa SIP (Dan et al., submitted for publication), unlike the plume-derived or asthenosphere-derived mafic rocks in the accretionary orogenesis and mafic large igneous provinces. Thus, remelting of the newly-formed mafic rocks in the mid-to-lower crust produced unradiogenic Nd isotopic compositions. Similar negative $\varepsilon_{Nd}(t)$ values from felsic igneous rocks are also prevalent in other SIPs, such as the Chon Aike SLIP (Riley et al., 2001) and the Mesoproterozoic Gawler SLIP, southern Australia (Wade et al., 2012), where mafic rocks were also mostly sourced from enriched lithospheric mantle.

7. Conclusions

Two stages of MMEs–host granitoids pairs (280 and 270 Ma) are recognized in the Alxa silicic igneous province (Alxa SIP), and each pair has similar whole rock Sr–Nd and zircon Hf–O isotopic compositions. The occurrence of quartz xenocrysts, K-feldspar megacrysts, corroded feldspars and acicular apatites indicates that the MMEs are the products of magma mixing. The striking resemblance of the zircon Hf–O isotopic compositions in both MMEs–host granitoids pairs indicates that the granitoids were mainly sourced from the magmas generated by partial remelting of mafic rocks in the mid-to-lower crust that had been emplaced slightly earlier by basaltic magma underplating or injection into crust. Pervasive basaltic magma underplating or injection into crust, followed by the remelting of these mafic rocks in the mid-to-lower crust due to continued basaltic magma intrusion, indicate an episode of substantial crustal growth occurred in the generation of the Alxa SIP.

Supplementary data to this article can be found online at http://dx.doi.org/10.1016/j.lithos.2015.05.016.

Acknowledgments

We thank X.H. Li for assistance in fieldwork, and Q.L. Li and G.Q. Tang for SIMS analyses. Thoughtful and constructive comments by two anonymous reviewers and editorial comments by S.L. Chung substantially improved the manuscript. This study was financially supported by the Strategic Priority Research Program (B) of the Chinese Academy of Sciences (grant no. XDB03010600), Major State Basic Research Program (973 Program) of the People's Republic of China (grant no. 2011CB808906), National Natural Science Foundation of China (grant nos. 41025006, 41303018 and 41421062), China Postdoctoral Science Foundation (grant no. 2013M531880), and the Guangzhou Institute of Geochemistry, Chinese Academy of Sciences (GIGCAS 135 project Y234021001). This is contribution no. IS-2085 from GIGCAS.

References

Allen, C.M., 1991. Local equilibrium of mafic enclaves and granitoids of the Turtle pluton, southeast California: mineral, chemical, and isotopic evidence. American Mineralogist 76, 574–588.
Annen, C., Sparks, R.S.J., 2002. Effects of repetitive emplacement of basaltic intrusions on thermal evolution and melt generation in the crust. Earth and Planetary Science Letters 203, 937–955.
Annen, C., Blundy, J.D., Sparks, R.S.J., 2006. The genesis of intermediate and silicic magmas in deep crustal hot zones. Journal of Petrology 47, 505–539.
Appleby, S.K., Graham, C.M., Gillespie, M.R., Hinton, R.W., Oliver, G.J.H., EIMF, 2008. A cryptic record of magma mixing in diorites revealed by high-precision SIMS oxygen isotope analysis of zircons. Earth and Planetary Science Letters 269, 105–117.
Atherton, M.P., Petford, N., 1993. Generation of sodium-rich magmas from newly underplated basaltic crust. Nature 362, 144–146.
Barbarin, B., 2005. Mafic magmatic enclaves and mafic rocks associated with some granitoids of the central Sierra Nevada batholith, California: nature, origin, and relations with the hosts. Lithos 80, 155–177.
Bea, F., 1996. Residence of REE, Y, Th and U in granite and crustal protoliths; implications for the chemistry of crustal melts. Journal of Petrology 37, 521–552.
Belousova, E.A., Griffin, W.L., O'Reilly, S.Y., Fisher, N.I., 2002. Igneous zircon: trace element composition as an indicator of source rock type. Contributions to Mineralogy and Petrology 143, 602–622.
Blundy, J.D., Sparks, R.S.J., 1992. Petrogenesis of mafic inclusions in granitoids of the Adamello Massif, Italy. Journal of Petrology 33, 1039–1104.
Bonin, B., 1991. In: Didier, J., Barbarin, B. (Eds.), The Enclaves of the Alkaline Anorogenic Granites: An Overview. Enclaves and Granite Petrology. Developments in Petrology 13. Elsevier, Amsterdam, pp. 179–189.
Bonin, B., 2004. Do coeval mafic and felsic magmas in post-collisional to within-plate regimes necessarily imply two contrasting, mantle and crust, sources? A review. Lithos 78, 1–24.
Borg, L.E., Clynne, M.A., 1998. The petrogenesis of felsic calcalkaline magmas from the southernmost Cascades, California: origin by partial melting of basaltic lower crust. Journal of Petrology 39, 1197–1222.
Bryan, S., 2007. Silicic large igneous provinces. Episodes 30, 20–31.
Bryan, S.E., Ferrari, L., 2013. Large igneous provinces and silicic large igneous provinces: progress in our understanding over the last 25 years. Geological Society of America Bulletin 125, 1053–1078.
Bryan, S.E., Riley, T.R., Jerram, D.A., Stephens, C.J., Leat, P.T., 2002. Silicic volcanism: an undervalued component of large igneous provinces and volcanic rifted margins. In: Menzies, M.A., Klemperer, S.L., Ebinger, C.J., Baker, J. (Eds.), Volcanic Rifted Margins. Geological Society of America Special Paper 362, pp. 97–118.
Bryan, S.E., Ferrari, L., Reiners, P.W., Allen, C.M., Petrone, C.M., Ramos Rosique, A., Campbell, I.H., 2008. New insights into crustal contributions to large volume rhyolite generation at the mid-Tertiary Sierra Madre Occidental Province, Mexico, revealed by U–Pb geochronology. Journal of Petrology 49, 47–77.
Chappell, B.W., White, A.J.R., 1991. In: Didier, J., Barbarin, B. (Eds.), Restite Enclaves and the Restite Model. Developments in Petrology 13. Elsevier, Amsterdam, pp. 375–381.
Chappell, B.W., Wyborn, D., 2012. Origin of enclaves in S-type granites of the Lachlan Fold Belt. Lithos 154, 235–247.
Chappell, B.W., White, A.J.R., Wyborn, D., 1987. The importance of residual source material restite in granite petrogenesis. Journal of Petrology 28, 1111–1138.
Chung, S.L., Liu, D.Y., Ji, J.Q., Chu, M.F., Lee, H.Y., Wen, D.J., Lo, C.H., Lee, T.Y., Qian, Q., Zhang, Q., 2003. Adakites from continental collision zones: melting of thickened lower crust beneath southern Tibet. Geology 31, 1021–1024.
Collins, W.J., 1998. Evaluation of petrogenetic models for Lachlan Fold Belt granitoids: implications for crustal architecture and tectonic models. Australian Journal of Earth Science 45, 483–500.

Collins, W.J., Wiebe, R.A., Healy, B., Richards, S.W., 2006. Replenishment, crystal accumulation and floor aggradation in the megacrystic Kameruka Suite, Australia. Journal of Petrology 47, 2073–2104.
Dahlquist, J.A., 2002. Mafic microgranular enclaves: early segregation from metaluminous magma (Sierra de Chepes), Pampean Ranges, NW Argentina. Journal of South American Earth Sciences 15, 643–655.
Dan, W., Li, X.H., Guo, J.H., Liu, Y., Wang, X.C., 2012. Paleoproterozoic evolution of the eastern Alxa Block, westernmost North China: evidence from in situ zircon U–Pb dating and Hf–O isotopes. Gondwana Research 21, 838–864.
Dan, W., Li, X.H., Wang, Q., Tang, G.J., Liu, Y., 2014a. The Early Permian (ca. 280 Ma) silicic igneous province in Alxa Block, NW China: a magmatic flare-up triggered by a mantle–plume? Lithos 204, 144–158.
Dan, W., Li, X.H., Wang, Q., Wang, X.C., Liu, Y., 2014b. Neoproterozoic S-type granites in the Alxa Block, westernmost north China and tectonic implications: in-situ zircon U–Pb–Hf–O isotopic and geochemical constraints. American Journal of Sciences 314, 110–153.
Dan, W., Li, X.H., Wang, Q., Tang, G.J., Liu, Y., Wyman, D.A., 2014c. Paleoproterozoic S-type granites in the Helanshan Complex, Khondalite Belt, North China Craton: implications for rapid sediment recycling during slab break-off. Precambrian Research 254, 59–72.
Dan, W., Li, X.H., Wang, Q., Wang, X.C., Liu, Y., 2015. Phanerozoic amalgamation of the Alxa Block and North China Craton: evidence from Paleozoic granitoids, U–Pb geochronology and Sr–Nd–Pb–Hf–O isotope geochemistry. Gondwana Research. http://dx.doi.org/10.1016/j.gr.2015.02.011.
Dan, W., Li, X.H., Wang, Q., Wang, X.C., Liu, Y., Dan, W., Li, X.H., Wang, Q., Wang, X.C., Liu, Y., 2015. Melting of Metasomatized Lithosphere Mantle in the Alxa Silicic Igneous Province: Evidence From the Middle Permian Mafic Rocks in the Alxa Block, NW China (submitted for publication).
Deering, C.D., Bachmann, O., Dufek, J., Gravley, D.M., 2011. Rift-related transition from andesite to rhyolite volcanism in the Taupo Volcanic Zone (New Zealand) controlled by crystal-melt dynamics in mush zones with variable mineral assemblages. Journal of Petrology 52, 2243–2263.
Didier, D., Barbarin, B., 1991. Enclaves and Granite Petrology, Developments in Petrology. Elsevier Science Publications, Amsterdam, pp. 1–625.
Dodge, F.C.W., Kistler, R.W., 1990. Some additional observations on inclusions in the granitic rocks of the Sierra Nevada. Journal of Geophysical Research 95, 17841–17848.
Donaire, T., Pascual, E., Pin, C., Duthou, J.L., 2005. Microgranular enclaves as evidence of rapid cooling in granitoid rocks: the case of the Los Pedroches granodiorite, Iberian Massif, Spain. Contributions to Mineralogy and Petrology 149, 247–265.
Dorais, M.J., Whitney, J.A., Roden, M.F., 1990. Origin of mafic enclaves in the Dinkey Creek Pluton, Central Sierra Nevada Batholith, California. Journal of Petrology 31, 853–881.
Eberz, G.W., Nicholls, I.A., 1990. Chemical modification of enclave magma by post-emplacement crystal fractionation, diffusion and metasomatism. Contributions to Mineralogy and Petrology 104, 47–55.
Ernst, R.E., 2014. Large Igneous Provinces. Cambridge University Press (653 pp.).
Esna-Ashari, A., Hassanzadeh, J., Valizadeh, M., 2011. Geochemistry of microgranular enclaves in Aligoodarz Jurassic arc pluton, western Iran: implications for enclave generation by rapid crystallization of cogenetic granitoid magma. Mineralogy and Petrology 101, 195–216.
Feeley, T.C., Wilson, L.F., Underwood, S.J., 2008. Distribution and compositions magmatic inclusions in the Mount Helen dome, Lassen volcanic center, California: insights into magma chamber processes. Lithos 106, 173–189.
Frost, C.D., Bell, J.M., Frost, B.R., Chamberlain, K.R., 2001. Crustal growth by magmatic underplating: isotopic evidence from the northern Sherman batholith. Geology 29, 515–518.
Geng, Y.S., Wang, X.S., Shen, Q.H., Wu, C.M., 2007. Chronology of the Precambrian metamorphic series in the Alxa area, Inner Mongolia. Geology in China 34, 251–261 (in Chinese with English abstract).
Gong, J.H., Zhang, J.X., Yu, S.Y., 2011. The origin of Longshoushan Group and associated rocks in the southern part of the Alxa block: constraint from LA-ICP-MS U–Pb zircon dating. Acta Petrologica et Mineralogica 30, 795–818.
Gong, J.H., Zhang, J.X., Yu, S.Y., Li, H.K., Hao, K.J., 2012. The ~2.5 Ga TTG in the western Alxa Block and its geological significance. Science China Bulletin 57, 2715–2728.
Griffin, W.L., Wang, X., Jackson, S.E., Pearson, N.J., O'Reilly, S.Y., Xu, X.S., Zhou, X.M., 2002. Zircon chemistry and magmamixing, SE China: in-situ analysis of Hf isotopes, Tonglu and Pingtan igneous complexes. Lithos 61, 237–269.
Griffin, W.L., Pearson, N.J., Belousova, E.A., Saeed, A., 2006. Comment: Hf-isotope heterogeneity in zircon 91500. Chemical Geology 233, 358–363.
Hawkesworth, C.J., Turner, S.P., McDermott, F., Peate, D.W., van Calsteren, P., 1997. U–Th isotopes in arc magmas: implications for element transfer from the subducted crust. Science 276, 551–555.
Hibbard, M.J., 1991. Textural anatomy of twelve magma-mixed granitoid systems. In: Didier, J., Barbarin, B. (Eds.), Enclaves and Granite Petrology. Elsevier, Amsterdam, pp. 431–444.
Holden, P., Halliday, A.N., Stephens, W.E., Henney, P.J., 1991. Chemical and isotopic evidence for major mass transfer between mafic enclaves and felsic magma. Chemical Geology 92, 135–152.
Hu, Z.C., Liu, Y.S., Gao, S., Liu, W.G., Yang, L., Zhang, W., Tong, X.R., Lin, L., Zong, K.Q., Li, M., Chen, H.H., Zhou, L., Yang, L., 2012. Improved in situ Hf isotope ratio analysis of zircon using newly designed X skimmer cone and Jet sample cone in combination with the addition of nitrogen by laser ablation multiple collector ICP-MS. Journal of Analytical Atomic Spectrometry 27, 1391–1399.
Jahn, B.M., Wu, F.Y., Chen, B., 2000. Massive granitoid generation in Central Asia: Nd isotope evidence and implication for continental growth in the Phanerozoic. Episodes 23, 82–92.
Johnson, K., Barnes, C.G., Miller, C.A., 1997. Petrology, geochemistry, and genesis of high-Al tonalite and trondhjemites of the Cornucopia Stock, Blue Mountains, Northeastern Oregon. Journal of Petrology 38, 1585–1611.
Kemp, A.I.S., Hawkesworth, C.J., Foster, G.L., Paterson, B.A., Woodhead, J.D., Hergt, J.M., Gray, C.M., Whitehouse, M.J., 2007. Magmatic and crustal differentiation history of granitic rocks from Hf–O isotopes in zircon. Science 315, 980–983.
Lesher, C.E., 1990. Decoupling of chemical and isotopic exchange during magma mixing. Nature 344, 235–237.
Li, J.J., 2006. Regional Metallogenic System of Alashan Block in Inner Mongolia Autonomous Region. China University of Geosciences, Beijing (Ph.D. thesis, 177p).
Li, X.H., Sun, M., Wei, G.J., Liu, Y., Lee, C.Y., Malpas, J., 2000. Geochemical and Sm–Nd isotopic study of amphibolites in the Cathaysia Block, southeastern China: evidence for an extremely depleted mantle in the Paleoproterozoic. Precambrian Research 102, 251–262.
Li, X.H., Liu, D.Y., Sun, M., Li, W.X., Liang, X.R., Liu, Y., 2004. Precise Sm–Nd and U–Pb isotopic dating of the supergiant Shizhuyuan polymetallic deposit and its host granite, SE China. Geological Magazine 141, 225–231.
Li, X.H., Qi, C.S., Liu, Y., Liang, X.R., Tu, X.L., Xie, L.W., Yang, Y.H., 2005. Petrogenesis of the Neoproterozoic bimodal volcanic rocks along the western margin of the Yangtze Block: new constraints from Hf isotopes and Fe/Mn ratios. Chinese Science Bulletin 50, 2481–2486.
Li, X.H., Liu, Y., Li, Q.L., Guo, C.H., Chamberlain, K.R., 2009. Precise determination of Phanerozoic zircon Pb/Pb age by multicollector SIMS without external standardization. Geochemistry, Geophysics, Geosystems 10, Q04010. http://dx.doi.org/10.1029/2009GC002400.
Li, X.H., Li, W.X., Li, Q.L., Wang, X.C., Liu, Y., Yang, Y.H., 2010a. Petrogenesis and tectonic significance of the similar to 850 Ma Gangbian alkaline complex in South China: evidence from in situ zircon U–Pb dating, Hf–O isotopes and whole-rock geochemistry. Lithos 114, 1–15.
Li, X.H., Long, W.G., Li, Q.L., Liu, Y., Zheng, Y.F., Yang, Y.H., Chamberlain, K.R., Wan, D.F., Guo, C.H., Wang, X.C., Tao, H., 2010b. Penglai zircon megacrysts: a potential new working reference material for microbeam determination of Hf–O isotopes and U–Pb age. Geostandards and Geoanalytical Research 34, 117–134.
Li, S.Q., Hegner, E., Yang, Y.Z., Wu, J.D., Chen, F.K., 2014. Age constraints on late Mesozoic lithospheric extension and origin of bimodal volcanic rocks from the Hailar basin, NE China. Lithos 190–191, 204–219.
Liu, L., Qiu, J.S., Li, Z., 2013. Origin of mafic microgranular enclaves (MMEs) and their host quartz monzonites from the Muchen pluton in Zhejiang Province, Southeast China: implications for magma mixing and crust–mantle interaction. Lithos 160–161, 145–163.
Ludwig, K.R., 2003. Users manual for Isoplot 3.00: a geochronological toolkit for Microsoft Excel. Special, Publication 4. Berkeley Geochronology Center.
Middlemost, E.A.K., 1994. Naming materials in the magma/igneous rock system. Earth-Science Reviews 37, 215–224.
Neves, S.P., Mariano, G., Guimarães, I.P., da Silva Filho, A.F., Melo, S.C., 2000. Intralithospheric differentiation and crustal growth: evidence from the Borborema province, northeastern Brazil. Geology 28, 519–522.
NMBGMR (Nei Mongol Bureau of Geology and Mineral Resources), 1991. Regional Geology of Nei Mongol Autonomous Region. Geological Publishing House, Beijing (725p (in Chinese with English abstract)).
Pascual, E., Donaire, T., Pin, C., 2008. The significance of microgranular enclaves in assessing the magmatic evolution of a high-level composite batholith: a case on the Los Pedroches Batholith, Iberian Massif, Spain. Geochemical Journal 42, 177–198.
Peccerillo, R., Taylor, S.R., 1976. Geochemistry of Eocene calc-alkaline volcanic rocks from the Kastamonu area, northern Turkey. Contributions to Mineralogy and Petrology 58, 63–81.
Petford, N., Atherton, M., 1996. Na-rich partial melts from newly underplated basaltic crust: the Cordillera Blanca Batholith, Peru. Journal of Petrology 37, 1491–1521.
Petford, N., Gallagher, K., 2001. Partial melting of mafic (amphibolitic) lower crust by periodic influx of basaltic magma. Earth and Planetary Science Letters 193, 483–499.
Quick, J.E., Sinigoi, S., Peressini, G., Demarchi, G., Wooden, J.L., Sbisà, A., 2009. Magmatic plumbing of a large Permian caldera exposed to a depth of 25 km. Geology 37, 603–606.
Riley, T.R., Leat, P.T., Pankhurst, R.J., Harris, C., 2001. Origins of large volume rhyolitic volcanism in the Antarctic Peninsula and Patagonia by crust melting. Journal of Petrology 42, 1043–1065.
Rooney, T.O., Deering, C.D., 2014. Conditions of melt generation beneath the Taupo Volcanic Zone: the influence of heterogeneous mantle inputs on large-volume silicic systems. Geology 42, 3–6.
Sengör, A.M.C., Natal'in, B.A., Burtman, V.S., 1993. Evolution of the Altaid tectonic collage and Palaeozoic crustal growth in Eurasia. Nature 364, 299–307.
Shellnutt, J.G., Jahn, B.M., Dostal, J., 2010. Elemental and Sr–Nd isotope geochemistry of microgranular enclaves from peralkaline A-type granitic plutons of the Emeishan large igneous province, SW China. Lithos 119, 34–46.
Silva, M.M.V.G., Neiva, A.M.R., Whitehouse, M.J., 2000. Geochemistry of enclaves and host granite from the Nelas area, central Portugal. Lithos 50, 153–170.
Sinigoi, S., Quick, J.E., Demarchi, G., Kloetzli, U., 2011. The role of crustal fertility in the generation of large silicic magmatic systems triggered by intrusion of mantle magma in the deep crust. Contributions to Mineralogy and Petrology 162, 691–707.
Sun, S.S., McDonough, W.F., 1989. Chemical and isotopic systematics of oceanic basalt: implications for mantle composition and processes. In: Sanders, A.D., Norry, M.J. (Eds.), Magmatism in the Ocean Basins. Geological Society Special Publication 42, pp. 528–548.
Sun, J.F., Yang, J.H., Wu, F.Y., Li, X.H., Yang, Y.H., Xie, L.W., Wilde, S.A., 2010. Magma mixing controlling the origin of the Early Cretaceous Fangshan granitic pluton, North China Craton: in situ U–Pb age and Sr-, Nd-, Hf- and O-isotope evidence. Lithos 120, 421–438.

Tang, G.J., Wang, Q., Wyman, D.A., Li, Z.-X., Zhao, Z.-H., Yang, Y.H., 2012. Late Carboniferous high $\varepsilon_{Nd}(t)$–$\varepsilon_{Hf}(t)$ granitoids, enclaves and dikes in western Junggar, NW China: ridge-subduction-related magmatism and crustal growth. Lithos 140–141, 85–101.
Tindle, A.G., 1991. Trace element behavior in microgranular enclaves from granitic rocks. In: Didier, J., Barbarin, B. (Eds.), Enclaves and Granite Petrology. Elsevier, Amsterdam, pp. 313–331.
Tindle, A.G., Pearce, J.A., 1983. Assimilation and partial melting of continental crust: evidence from the mineralogy and geochemistry of autoliths and xenoliths. Lithos 16, 185–202.
Valley, J.W., Kinny, P.D., Schulze, D.J., Spicuzza, M.J., 1998. Zircon megacrysts from kimberlite: oxygen isotope variability among mantle melts. Contributions to Mineralogy and Petrology 133, 1–11.
Vernon, R.H., 1984. Microgranitoid enclaves in granites: globules of hybrid magma quenched in a plutonic environment. Nature 309, 438–439.
Vernon, R.H., 1990. Crystallization and hybridism in microgranitoid enclave magmas: microstructural evidence. Journal of Geophysical Research 95 (B11), 17849–17859.
Vernon, R.H., 2007. Problems in identifying restite in granites of southeastern Australia, with speculations on sources of magma and enclaves. Canadian Mineralogist 45, 147–178.
Wade, C.E., Reid, A.J., Wingate, M.T.D., Jagodzinski, E.A., Barovich, K., 2012. Geochemistry and geochronology of the c. 1585 Ma Benagerie Volcanic Suite, southern Australia: relationship to the Gawler Range Volcanics and implications for the petrogenesis of a Mesoproterozoic silicic large igneous province. Precambrian Research 206–207, 17–35.
Wang, Q., McDermott, F., Xu, J.F., Bellon, H., Zhu, Y.T., 2005. Cenozoic K-rich adakitic volcanic rocks in the Hohxil area, northern Tibet: lower-crustal melting in an intracontinental setting. Geology 33, 465–468.
Wang, Q., Xu, J.F., Jian, P., Bao, Z.W., Zhao, Z.H., Li, C.F., Xiong, X.L., Ma, J.L., 2006a. Petrogenesis of adakitic porphyries in an extensional tectonic setting, Dexing, South China: implications for the genesis of porphyry copper mineralization. Journal of Petrology 47 (1), 119–144.
Wang, X.C., Liu, Y.S., Liu, X.M., 2006b. Mesozoic adakites in the Lingqiu Basin of the central North China Craton: partial melting of underplated basaltic lower crust. Geochemical Journal 40, 447–461.
Wang, Q., Li, X.H., Jia, X.H., Wyman, D.A., Tang, G.J., Li, Z.X., Yang, Y.H., Jiang, Z.Q., Ma, L., Gou, G.N., 2012. Late Early Cretaceous adakitic granitoids and associated magnesian and potassium-rich mafic enclaves and dikes in the Tunchang–Fengmu area, Hainan Province (South China): partial melting of lower crust and mantle, and magma hybridization. Chemical Geology 328, 222–243.
White, A.J.R., Chappell, B.W., Wyborn, D., 1999. Application of the restite model to the Deddick granodiorite and its enclaves—a reinterpretation of the observations and data of Maas et al. Journal of Petrology 40, 413–421.
Wiebe, R.A., Smith, D., Sturn, M., King, E.M., 1997. Enclaves in the Cadillac mountain granite (Coastal Maine): samples of hybrid magma from the base of the chamber. Journal of Petrology 38, 393–426.
Wiedenbeck, M., Hanchar, J.M., Peck, W.H., Sylvester, P., Valley, J., Whitehouse, M., Kronz, A., Morishita, Y., Nasdala, L., Fiebig, J., Franchi, I., Girard, J.P., Greenwood, R.C., Hinton, R., Kita, N., Mason, P.R.D., Norman, M., Ogasawara, M., Piccoli, R., Rhede, D., Satoh, H., Schulz-Dobrick, B., Skar, O., Spicuzza, M.J., Terada, K., Tindle, A., Togashi, S., Vennemann, T., Xie, Q., Zheng, Y.F., 2004. Further characterisation of the 91500 zircon crystal. Geostandards and Geoanalystical Research 28, 9–39.
Wu, F.Y., Yang, Y.H., Xie, L.W., Yang, J.H., Xu, P., 2006. Hf isotopic compositions of the standard zircons and baddeleyites used in U–Pb geochronology. Chemical Geology 234, 105–126.
Xu, Y.G., Luo, Z.Y., Huang, X.L., He, B., Xiao, L., Xie, L.W., Shi, Y.R., 2008. Zircon U–Pb and Hf isotope constraints on crustal melting associated with the Emeishan mantle plume. Geochimica et Cosmochimica Acta 72, 3084–3104.
Yang, J.H., Wu, F.Y., Chung, S.L., Wilde, S.A., Chu, M.F., 2006. A hybrid origin for the Qianshan A-type granite, northeast china: geochemical and Sr–Nd–Hf isotopic evidence. Lithos 89, 89–106.
Yang, J.H., Wu, F.Y., Wilde, S.A., Xie, L.W., Yang, Y.H., Liu, X.M., 2007. Trace magma mixing in granite genesis: in-situ U–Pb dating and Hf-isotope analysis of zircons. Contributions to Mineralogy and Petrology 153, 177–190.
Zeh, A., Gerdes, A., Klemd, R., Barton, J.M., 2007. Archaean to Proterozoic Crustal evolution in the Central Zone of the Limpopo Belt (South Africa–Botswana): constraints from combined U–Pb and Lu–Hf isotope analyses of zircon. Journal of Petrology 48, 1605–1639.
Zhang, J.J., Wang, T., Zhang, Z.C., Tong, Y., Zhang, L., 2012. Magma mixing origin of Yamatu granite in Nuoergong–Langshan area, western part of the northern margin of North China Craton: petrological and geochemical evidences. Geological Review 58, 53–66.
Zhang, J.X., Gong, J.H., Yu, S.Y., Li, H.K., Hou, K.J., 2013. Neoarchean–Paleoproterozoic multiple tectonothermal events in the western Alxa block, North China Craton and their geological implication: evidence from zircon U–Pb ages and Hf isotopic composition. Precambrian Research 235, 36–57.
Zhao, G.C., 2014. Precambrian Evolution of the North China Craton. Elsevier, Amsterdam (194 pp.).
Zhao, G.C., Cawood, P.A., 2012. Precambrian geology of China. Precambrian Research 222–223, 13–54.
Zhao, G.C., Sun, M., Wilde, S.A., Li, S.Z., 2005. Late Archean to Paleoproterozoic evolution of the North China Craton: key issues revisited. Precambrian Research 136, 177–202.
Zhao, J.H., Zhou, M.F., Zheng, J.P., 2013. Neoproterozoic high-K granites produced by melting of newly formed mafic crust in the Huangling region, South China. Precambrian Research 233, 93–107.
Zhong, H., Campbell, I.H., Zhu, W.-G., Allen, C.M., Hu, R.-Z., Xie, L.-W., He, D.-F., 2011. Timing and source constraints on the relationship between mafic and felsic intrusions in the Emeishan large igneous province. Geochimica et Cosmochimica Acta 75, 1374–1395.
Zi, J.W., Cawood, P.A., Fan, W.M., Tohver, E., Wang, Y.J., McCuaig, T.C., 2012. Generation of Early Indosinian enriched mantle-derived granitoid pluton in the Sanjiang Orogen (SW China) in response to closure of the Paleo-Tethys. Lithos 140–141, 166–182.